Molecular Biology of the Cell
Vol. 20, 1302–1311, March 1, 2009

The Novel Adaptor Protein Tks4 (SH3PXD2B) Is Required for Functional Podosome Formation

Matthew D. Buschman,*† Paul A. Bromann,*‡§ Pilar Cejudo-Martin,*‡ Fang Wen,* Ian Pass,* and Sara A. Courtneidge*

*Tumor Microenvironment Program, Burnham Institute for Medical Research, La Jolla, CA 92037; and †Molecular Pathology Graduate Program, University of California, San Diego, La Jolla, CA 92093

Submitted September 18, 2008; Revised November 25, 2008; Accepted January 5, 2009
Monitoring Editor: Joan Brugge

Metastatic cancer cells have the ability to both degrade and migrate through the extracellular matrix (ECM). Invasiveness can be correlated with the presence of dynamic actin-rich membrane structures called podosomes or invadopodia. We showed previously that the adaptor protein tyrosine kinase substrate with five Src homology 3 domains (Tks5)/Fish is required for podosome/invadopodia formation, degradation of ECM, and cancer cell invasion in vivo and in vitro. Here, we describe Tks4, a novel protein that is closely related to Tks5. This protein contains an amino-terminal Phox homology domain, four SH3 domains, and several proline-rich motifs. In Src-transformed fibroblasts, Tks4 is tyrosine phosphorylated and predominantly localized to rosettes of podosomes. We used both short hairpin RNA knockdown and mouse embryo fibroblasts lacking Tks4 to investigate its role in podosome formation. We found that lack of Tks4 resulted in incomplete podosome formation and inhibited ECM degradation. Both phenotypes were rescued by reintroduction of Tks4, whereas only podosome formation, but not ECM degradation, was rescued by overexpression of Tks5. The tyrosine phosphorylation sites of Tks4 were required for efficient rescue. Furthermore, in the absence of Tks4, membrane type-1 matrix metalloproteinase (MT1-MMP) was not recruited to the incomplete podosomes. These findings suggest that Tks4 and Tks5 have overlapping, but not identical, functions, and implicate Tks4 in MT1-MMP recruitment and ECM degradation.

INTRODUCTION

In recent years, there has been increasing interest in defining the mechanisms by which cancer cells acquire invasive behavior. In particular, dynamic membrane structures called podosomes or invadopodia have been shown to play an important role in invasive cell motility and extracellular matrix (ECM) degradation (reviewed in Linder, 2007; Gimona *et al*., 2008). Invadopodia are actin-rich membrane protrusions that coordinate the cytoskeleton with extracellular proteolysis. Invadopodia have been found in many different types of invasive human cancer cells, and they are particularly well studied in breast cancer and melanoma as well as Src-transformed fibroblasts, in which they were first discovered (Chen *et al*., 1985; Tarone *et al*., 1985; Chen and Wang, 1999).

Several normal cell types whose physiological roles require motility and ECM degradation can also form podosomes (Linder and Aepfelbacher, 2003). This list includes osteoclasts, macrophages, endothelial cells, and vascular smooth muscle cells. Current convention is to call the structures that exist in normal cells and in Src-transformed cells podosomes, and to use the term invadopodia for those structures found in invasive cancer cells (Gimona *et al*., 2008). Although some investigators have noted structural differences between podosomes and invadopodia, few molecular differences have been described. This leaves open the possibility that differences in culture conditions may influence podosome/invadopodia architecture and function. Indeed, a recent article reported that extracellular matrix rigidity influences both the number and activity of invadopodia (Alexander *et al*., 2008). Our understanding of the protein components of podosomes and invadopodia has deepened in recent years, and we are also beginning to learn the signals that promote the formation and turnover of these structures. Ultimately, the study of both podosomes and invadopodia may yield new targets for cancer therapeutics.

Many of the original studies on podosomes/invadopodia were conducted in Src-transformed fibroblasts, and this continues to be a rich model system to study their structure and function. These cells are highly invasive both in vitro and in vivo, and the podosomes are abundant and arranged in characteristic rings known as rosettes. Furthermore, several lines of evidence point to a physiological role for Src in both podosome and invadopodia formation. For example, mice lacking Src develop osteopetrosis because of a podosome defect of osteoclasts (Soriano *et al*., 1991; Boyce *et al*., 1992; Lowe *et al*., 1993). The transforming growth factor-β–stimulated podosome formation seen in aortic endothelial cells requires Src (Varon *et al*., 2006). And Src is also required for

This article was published online ahead of print in *MBC in Press* (http://www.molbiolcell.org/cgi/doi/10.1091/mbc.E08–09–0949) on January 14, 2009.

‡ These authors contributed equally to this work.

§ Present address: Molecular Cancer Biology Program, Biomedicum Helsinki, P.O. Box 63, Haartmaninkatu 8, 00014 Helsinki, Finland.

Address correspondence to: Sara A. Courtneidge (courtneidge@burnham.org).

Abbreviations used: ECM, extracellular matrix; GFP, green fluorescent protein; GST, glutathione transferase; MEF, mouse embryo fibroblast; PCR, polymerase chain reaction; PX, Phox homology; Tks5, tyrosine kinase substrate with 5 SH3 domains.

invadopodia formation in human breast cancer cells (Artym *et al*., 2006; Cortesio *et al*., 2008). In keeping with a role for Src in podosome/invadopodia formation, many Src substrates are obligate podosome components, including cortactin, AFAP110, paxillin, p130Cas, ASAP1, and dynamin (Baldassarre *et al*., 2003; Brabek *et al*., 2004; Gatesman *et al*., 2004; Webb *et al*., 2006; Bharti *et al*., 2007; Clark *et al*., 2007; Badowski *et al*., 2008).

Some years ago, we cloned a new Src substrate, and we showed that it localized to podosomes of Src-transformed fibroblasts (Lock *et al*., 1998; Abram *et al*., 2003). We originally called this protein Fish, but we now designate it as tyrosine kinase substrate with five Scr homology 3 (SH3) domains (Tks5, gene symbol SH3PXD2A), Tks5 is a large adaptor or scaffold protein with an amino-terminal Phox homology or PX domain, and five SH3 domains. It also contains several proline-rich motifs and at least two Src phosphorylation sites. Our subsequent experiments using short hairpin RNA (shRNA)-mediated reduction in Tks5 expression in Src-transformed fibroblasts (Src-3T3) showed that it is required for podosome formation, ECM degradation, and invasion through Matrigel (Seals *et al*., 2005). We also found that Tks5 is overexpressed in several human cancer cell lines and tissues. Knockdown of Tks5 in melanoma and breast cancer cells results in decreased protease-dependent invasion. Furthermore, expression of Tks5 in a noninvasive breast cancer cell line results in the formation of invadopodia (Seals *et al*., 2005). Together, these data suggest that Tks5 is an essential scaffold protein of podosomes/invadopodia. We went on to test the tumorigenicity of Src-3T3 cells with and without Tks5 knockdown (Blouw *et al*., 2008). We found that tumor growth of the Tks5 knockdowns is inhibited regardless of whether tumor cells are introduced subcutaneously or intravenously (to give rise to experimental lung metastases). The most obvious defects in the tumors arising from the knockdown cells is a poorly developed tumor vasculature. These data are consistent with a role of Tks5, and perhaps by implication, podosomes/invadopodia, in tumor growth in vivo. We are currently investigating whether Tks5 is required for proteolytic processing of vascular growth factors in the tumor microenvironment.

Because Tks5 has no catalytic activity, it is likely to act by bringing together key regulators of podosomes/invadopodia. We have shown previously that its PX domain, which binds phosphatidylinositol-3,4-bisphosphate (PI-3,4P_2) and phosphatidylinositol-3-phosphate (PI 3-P), is required for the generation of podosomes/invadopodia (Abram *et al*., 2003). The fifth SH3 domain of Tks5 binds the transmembrane metalloproteases ADAMs 12, 15, and 19 (Abram *et al*., 2003). More recently, it was shown that accumulation of PI-3,4P_2 at focal adhesions results in the recruitment of a Tks5–Grb2 complex (Oikawa *et al*., 2008). Subsequent binding of neural Wiskott Aldrich syndrome protein (N-WASp) to Tks5 facilitates formation of rosettes of podosomes in Src-transformed fibroblasts.

When we originally cloned Tks5, which is encoded by the SH3PXD2A gene on human chromosome 10, a search of available databases revealed no closely homologous sequences. The nearest relative to Tks5 was p47phox, a component of the NADPH oxidase system of phagocytic cells, which has one PX domain and two SH3 domains, arranged in a similar orientation to Tks5. More recently, however, in a search of cDNA databases we found a sequence (derived from a mouse dendritic cell cDNA library) that more closely resembled Tks5 and that we called Tks4 (Courtneidge *et al*., 2005). Here, we describe our identification and initial characterization of this gene product.

MATERIALS AND METHODS

Cloning of Tks4

To search for Tks5-related genes, a homology BLAST search of public databases was performed using the human Tks5 protein sequence. A human cDNA, FLJ46896 (clone UTERU3021231), was identified that had significant homology to the human Tks5 transcript. This cDNA encoded a hypothetical protein (accession no. LOC285590) that also had significant homology to the Tks5 protein. Subsequently, this hypothetical gene product has been annotated as SH3 and PX domains 2B (SH3PXD2B), with the putative human gene product NM_014631 and the putative mouse gene product NM_177364. Mouse RNA was purified from low passage NIH-3T3 cells by using TRIzol (Invitrogen, Carlsbad, CA) nucleotide extraction, and adult brain RNA was obtained from Stratagene (La-Jolla, CA). SuperScript II reverse transcriptase (Invitrogen) was used to generate mouse and human oligo(dT)-primed cDNA according to the manufacturer's instructions. To clone the full-length transcript, oligonucleotides were designed and used to amplify the appropriate full-length transcript from mouse as well as human cDNA by using Phusion DNA polymerase (New England Biolabs, Ipswich, MA). Polymerase chain reaction (PCR) products were then cloned into pCR2.1-TOPO vector (Invitrogen), and multiple clones sequenced and analyzed. The human and mouse Tks4 clones were 100% identical in sequence to human and mouse SH3PXD2B, respectively.

Antibodies

Tks4–glutathione transferase (GST) fusion constructs were synthesized by PCR using oligonucleotides containing specific restriction endonuclease sites. PCR products were cloned into pGEX bacterial expression plasmids (GE Healthcare, Piscataway, NJ), and plasmids were sequenced. Constructs were transformed into the BL21 (DE3) strain of *Escherichia coli* (Stratagene, La Jolla, CA). Tks4–GST fusion protein expression was induced with 1 mM isopropyl β-D-thiogalactoside for 3 h at 37°C. Shaking flask cultures were centrifuged at 6000 × *g* at 4°C for 15 min to pellet bacteria. Bacterial pellets were suspended in lysis buffer (phosphate-buffered saline [PBS] plus 0.1% Triton X-100, 1 mM dithiothreitol [DTT], 1 mM phenylmethylsulfonyl fluoride, and Complete protease inhibitor cocktail [Roche Diagnostics, Indianapolis, IN]) and sonicated for 1 min at 4°C. Lysates were centrifuged at 20,000 × *g* for 30 min at 4°C, and supernatants were collected. Tks4-GST in supernatants was purified using glutathione-Sepharose (GE Healthcare) affinity chromatography, and Tks4-GST was eluted using PBS with 10 mM reduced glutathione.

Two Tks4-specific antisera were generated in rabbits and affinity purified by Millipore Bioscience Research Reagents (Temecula, CA). Tks4-A was generated by immunizing rabbits with a purified mouse Tks4–GST fusion protein, corresponding to amino acids 257-477 (09-260; Millipore Bioscience Research Reagents). Tks4-B was generated by immunizing rabbits with a purified human Tks4 GST fusion protein, corresponding to amino acids 431-595 (09-267; Millipore Bioscience Research Reagents). Tks5 antibodies have been described previously (Lock *et al*., 1998). The following commercial antibodies were used: anti-cortactin (4F10), anti-phosphotyrosine (4G10), and anti-membrane type-1 matrix metalloproteinase (MT1-MMP) (Millipore Bioscience Research Reagents); anti-FLAG (M2), and anti-vinculin (hVIN-1) (Sigma-Aldrich, St. Louis, MO); and anti-green fluorescent protein (GFP) (Invitrogen). Alexa Fluor 680 goat anti-rabbit or anti-mouse antibodies were used for immunoblot analysis, and Alexa Fluor 488 or 594 goat anti-rabbit or anti-mouse antibodies and Alexa Fluor 488 or 564 phalloidin were used for immunofluorescence microscopy (Invitrogen).

Cell Culture and Transfection

NIH-3T3 (3T3) and Src-transformed NIH-3T3 (Src-3T3) cells have been described previously (Lock *et al*., 1998). Stable Tks4 knockdown Src-3T3 cells were created using the Mission shRNA vector TRCN0000105931 (Sigma-Aldrich). Src-3T3 cells were transfected with shRNA vectors by using calcium phosphate transfection. Drug-resistant colonies were selected for and maintained in media containing 10 μg/ml puromycin. Primary mouse embryonic fibroblasts (MEFs) were isolated from wild-type and Tks4$^{-/-}$ day e13 mouse embryo littermates derived from embryonic stem cells containing a gene trap in the Tks4 locus (Lexicon, The Woodlands, TX). The abdominal organs and brain were dissected out for genotyping, whereas the remaining embryo was digested in 0.05% trypsin-EDTA and then washed and plated in DMEM containing 10% fetal bovine serum. Src-transformed MEFs (Src-MEFs) were created using pBABE-puro SrcY530F retrovirus infection (Morgenstern and Land, 1990) of passage 1 or 2 MEFs and selected for using 5 μg/ml puromycin. Early passage B16-F10 mouse melanoma cells were a gift from Peter Lock (La Trobe University, Melbourne, Australia). These cells were transfected with Lipofectamine 2000 (Invitrogen) according to the manufacturer's protocol. All cells were maintained in DMEM (Mediatech, Manassas, VA) containing 10% fetal bovine serum and antibiotics in 10% CO_2.

Constructs

All point mutations were introduced to Tks4 constructs by using QuikChange II site-directed mutagenesis (Stratagene). The active Src pSGT-SrcY527F construct has been described previously (Erpel *et al*., 1995). Lentiviruses encoding

Tks4 and Tks5 were created by subcloning Tks4-GFP or Tks5-GFP from pEGFP-N1 constructs to SIN18.hPGK lentivirus vector. Lentiviral preparations were made by the virus core facility at the Burnham Institute for Medical Research (La Jolla, CA).

Expression Profiling

Quantitative-PCR (Q-PCR) primers were designed using Primer3 web-based analysis software and obtained from Integrated DNA Technologies DNA (San Diego, CA). Specificity of Q-PCR primers was verified by amplifying serial 10-fold dilutions of cDNA from NIH3T3 cells and resolving PCR products by using agarose gel electrophoresis. All oligonucleotides amplified a single band of the correct molecular weight across all dilutions. The Mouse MTC Multiple Tissue cDNA Panel I (Clontech, Mountain View, CA) was used as template for Q-PCR tissue expression profiling. TRIzol (Invitrogen) nucleotide extraction was used to isolate RNA from NIH-3T3 and Src-3T3 cells, and oligo(dT)-primed cDNA was generated using SuperScript II reverse transcriptase (Invitrogen). Q-PCR was performed using the SYBR-Green PCR Master Mix (Applied Biosystems, Foster City, CA) on an MX3000 real-time PCR thermal cycler (Stratagene). Transcript levels were determined by analyzing ΔC_t data, and relative mRNA expression levels were determined by comparison with transcript levels in NIH-3T3 cDNA.

Immunoprecipitation and Immunoblot Analysis

Cell lysates were prepared by washing cells twice with cold Tris-buffered saline (TBS) containing 100 μM Na_3VO_4 and 2 mM DTT and then lysed in 50 mM Tris-HCl, pH 7.5, 150 mM NaCl, 1% Triton X-100, 10 mM NaF, 100 μM Na_3VO_4, and 2 mM DTT lysis buffer containing dissolved complete Mini protease inhibitor tab (Roche Diagnostics). For immunoprecipitations, protein extracts were incubated with 1 μl of antibody or antiserum and 15 μl of packed protein A-Sepharose beads (Sigma-Aldrich) or protein G-agarose beads (Calbiochem, San Diego, CA) for 60 min at 4°C. Immunocomplexes were then washed five times in lysis buffer and once in TBS containing 100 μM Na_3VO_4 and 2 mM DTT. Extracts were then eluted from beads by using SDS sample buffer, boiled for 5 min, and separated by SDS-polyacrylamide gel electrophoresis (PAGE) on 7.5 or 10% Criterion gels (Bio-Rad, Hercules, CA). SDS-PAGE gels were then transferred to Hybond nitrocellulose membranes (GE Healthcare) by using TransBlot SD semidry transfer system (Bio-Rad).

Immunofluorescence Microscopy

Cells were grown for 20 h on glass coverslips. Cells were then fixed with 4% paraformaldehyde/PBS (Electron Microscopy Sciences, Hatfield, PA) for 20 min, permeabilized with 0.1% Triton X-100/PBS for 10 min, and blocked with 2.5% goat serum. Fixed cells were incubated with primary antibodies for 1 h, extensively washed with PBS, and incubated with secondary antibodies and phalloidin for 30 min. Coverslips were mounted using VECTASHIELD (Vector Laboratories, Burlingame, CA). All images were captured on an Axioplan-2 fluorescence microscope with an AxioCam HRm camera and were analyzed with Axiovision 3.0 software (Carl Zeiss, Thornwood, NY), except for Figure 7, B and C, for which confocal microscopy was used.

ECM Assay

Fluorescently labeled gelatin-coated coverslips were prepared as described previously (Blouw *et al*., 2008). Cells were incubated on labeled coverslips for 3–20 h and either fixed with 4% paraformaldehyde/PBS at room temperature for 20 min or with methanol for 5 min at −20°C.

Zymography

Conditioned media samples were prepared as described previously (Seals *et al*., 2005) and analyzed on 10% gelatin zymogram gels (Invitrogen) according to the manufacturer's protocol.

Protein–Lipid Overlay

Protein–lipid overlay assays were performed as described previously (Dowler *et al*., 1999; Abram *et al*., 2003) by using phosphoinositide (PIP) assays from Echelon Biosciences (Salt Lake City, UT).

RESULTS

Tks4, a New Member of the Tks Family of Adaptor Proteins

After our initial finding of a cDNA with sequence similarity to Tks5 from a mouse dendritic cell library (Courtneidge *et al*., 2005), we used public gene database searches to identify further cDNAs in both mouse and human libraries. Genomic databases were also used to map the gene to human chromosome 5, and mouse chromosome 11. The gene has now been given the symbol SH3PXD2B. It encodes a theoretical protein with one PX domain and four SH3 domains (Figure 1), which we propose to call Tks4, for tyrosine kinase sub-

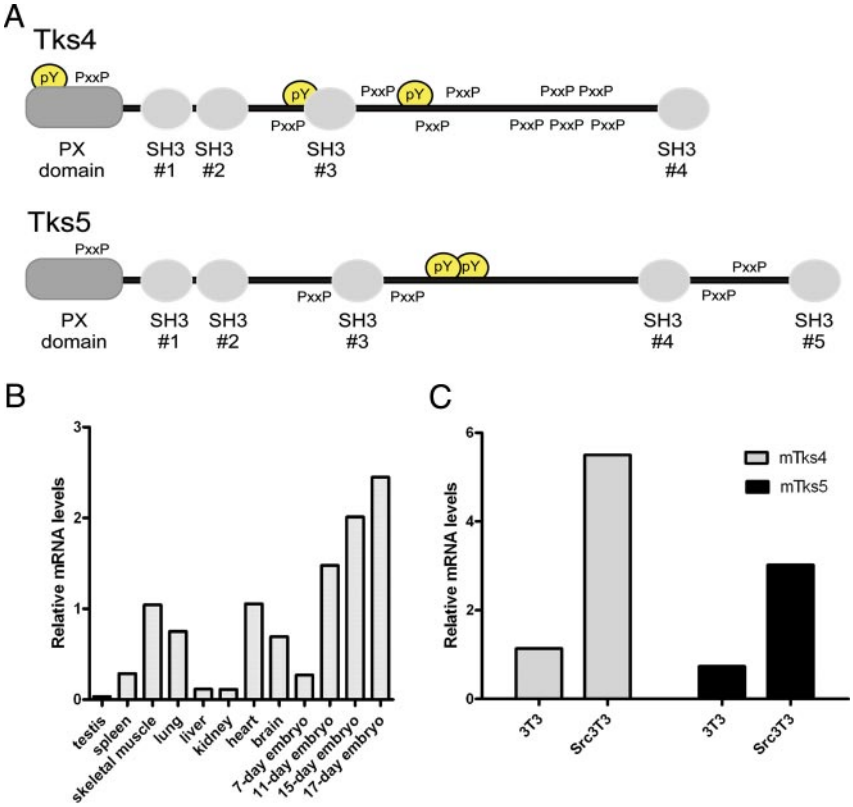

Figure 1. Topology and expression of Tks4. (A) The structures of Tks4 and Tks5 are shown. Dark gray boxes denote PX domains, and light gray boxes are SH3 domains. Proline-rich motifs are shown as PxxP, and phosphotyrosines as pY. (B) Tks4 mRNA levels were measured in a variety of mouse tissue samples by Q-PCR. Results are expressed relative to a value of 1 for 3T3 cells. (C) Tks4 and Tks5 mRNA levels were measured in 3T3 and Src-3T3 cells, by using 3T3 cells as the reference.

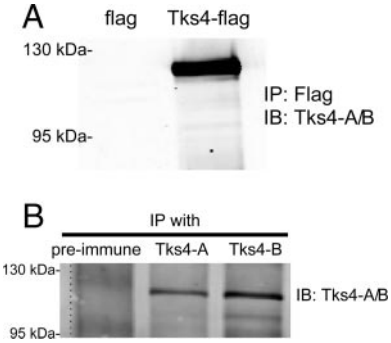

Figure 2. Molecular nature of Tks4 and antibody characterization. (A) Tks4-FLAG or empty-FLAG constructs were expressed in B16-F10 cells by transient transfection. Tks4-FLAG protein was immunoprecipitated with M2 anti-FLAG antibody and analyzed by SDS-PAGE and immunoblot analysis with Tks4-specific antisera. (B) Endogenous Tks4 protein was immunoprecipitated with either Tks4-A or Tks4-B antiserum from 3T3 cells and detected with a mixture of Tks4-A and Tks4-B antisera.

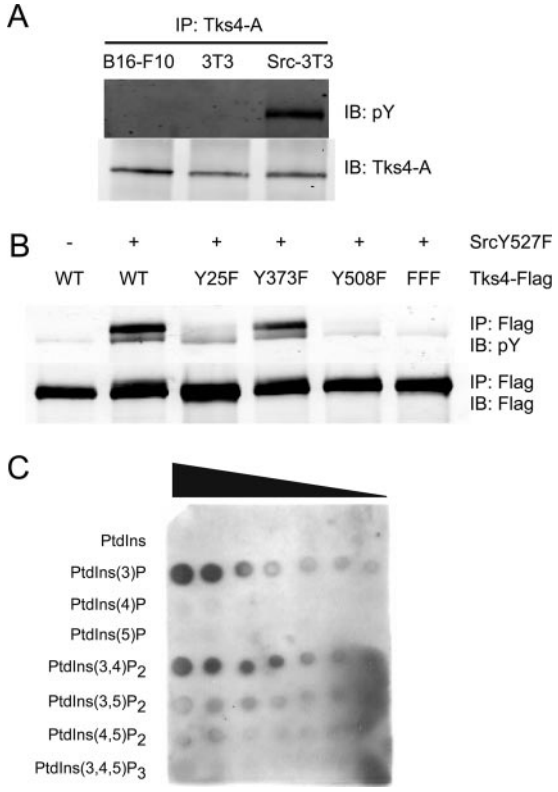

Figure 3. Tks4 can be tyrosine phosphorylated and its PX domain binds phosphatidylinositols. (A) Endogenous Tks4 protein was immunoprecipitated with Tks4-A antisera from B16-F10, 3T3, and Src-3T3 cells, analyzed by SDS-PAGE, and immunoblotted with a phosphotyrosine antibody. (B) Tyrosine-to-phenylalanine mutations were introduced into Tks4-FLAG by site-directed mutagenesis. Mutant and wild-type Tks4-FLAG constructs were coexpressed with Src in B16-F10 cells by transient transfection. Tks4-FLAG protein was immunoprecipitated with M2 anti-FLAG antibody, separated by SDS-PAGE, and detected by immunoblot analysis with anti-phosphotyrosine antibody. (C) Protein–lipid overlay assays were performed on a PIP array with GST-Tks4 PX domain fusion proteins. The phosphatidylinositols indicated are spotted left to right at doubling dilutions from 100 to 1.56 pmol/spot.

strate with four SH3 domains. Both Tks4 and Tks5 genes can be found in several species from fish (*Danio rerio*) to human. In simpler deuterostomes, however, there seems to be a single Tks gene. In the tunicate *Ciona intestinalis* this gene encodes a protein with one PX domain and three SH3 domains, whereas in the sea urchin *Strongylocentrotus purpuratus* the predicted product has one PX domain followed by four SH3 domains. Neither gene was found in organisms such as flies and worms. We subsequently cloned Tks4 from both a mouse NIH-3T3 cell and a human brain cDNA library, by using a PCR-based approach. The sequences of both clones closely matched the sequences in the databases.

When comparing the human genes, the overall identity between Tks4 and Tks5 is 43%. The PX domains share 77% identity, the first SH3 domains are 81% identical, the second are 68% identical, and the third are 70% identical. The fourth SH3 domain of Tks4 is most similar to the fifth SH3 domain of Tks5 (57% identity). The sequences between the SH3 domains, collectively called the linker sequences, are poorly conserved with only 12% overall identity. Thus, Tks4 most resembles Tks5 in its PX domain and SH3 domains. The fourth SH3 domain and surrounding linker sequences of Tks5 are not conserved in Tks4: in their place, Tks4 has a longer linker with several polyproline-rich motifs.

We used quantitative-PCR analysis on mouse tissues and cell lines to confirm that this hypothetical gene was transcribed. We found the highest transcript levels in embryonic samples, but there was also detectable expression in adult organs, including heart, spleen, brain, skeletal muscle, kidney, and liver. Both Tks4 and Tks5 were expressed in NIH-3T3 (3T3) cells, with Src transformation increasing the amount of each transcript three- to fivefold (Figure 1).

We next generated GST fusion proteins of linker sequences to use for the generation of antibodies. For the mouse gene, the linker between the second and third SH3 domains was used (Tks4-A). For the human sequence, we used the long linker between the third and fourth SH3 domains (Tks4-B). Antibodies were generated in rabbits and affinity purified by Millipore Bioscience Research Reagents. The antibodies were first tested on epitope-tagged Tks4 constructs and shown to both immunoprecipitate and immunoblot the transiently transfected protein (Figure 2). Note that Tks4, which has 911 amino acids and a predicted molecular mass of 101,553 Da, ran on SDS-polyacrylamide gels with an apparent molecular mass of 120 kDa. We also determined whether the antibodies could recognize endogenous protein. As shown in Figure 2, the antibodies also recognized a protein of 120 kDa from 3T3 cells. Presumably because of the sequence conservation between mouse and human Tks4 (90% in the linker between the second and third SH3 domains, 75% for that between third and fourth domains), both A and B antibodies recognized the mouse and human protein, both by immunoblotting and immunoprecipitation.

Phosphorylation and Lipid Binding Properties of Tks4

We have previously shown that Tks5 is a Src substrate, whose PX domain binds in vitro to the lipids PI 3-P and PI $3,4P_2$ (Abram *et al*., 2003). To determine whether Tks4 had similar properties, we first determined its phosphorylation status in vivo (Figure 3). We detected tyrosine phosphorylation of Tks4 in the Src-3T3 cells compared with parental 3T3s. Furthermore, coexpression of Src and Tks4 by transient transfection resulted in robust phosphorylation of Tks4, suggesting that it might be a direct substrate of Src. To map the tyrosine phosphorylation sites, we used site-di-

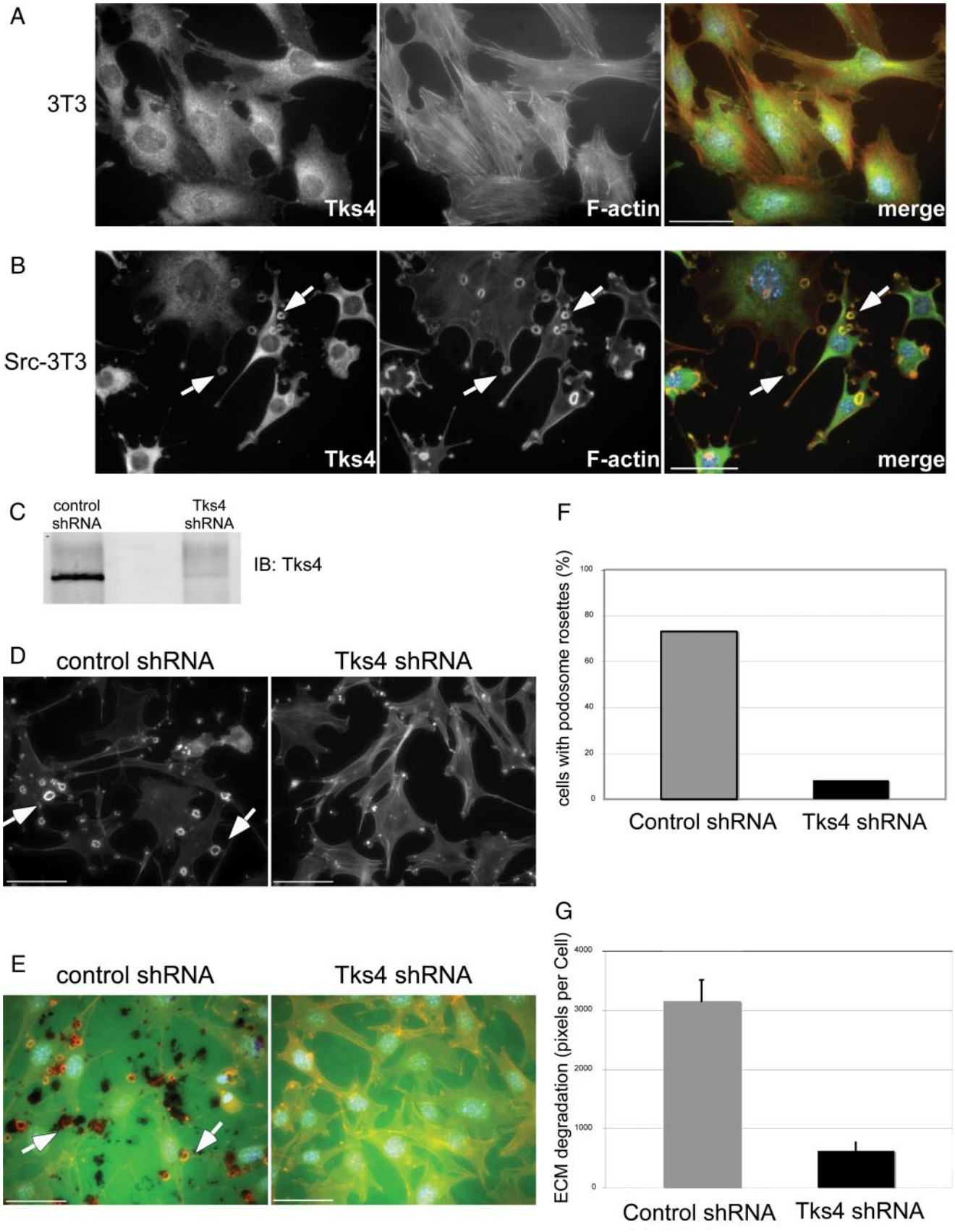

Figure 4. Tks4 localizes to podosomes and is required for their formation and function. (A) 3T3 were plated on glass coverslips for 20 h, fixed, and stained with Tks4 antiserum (green) and phalloidin (red). Bars, 50 μM. (B) Src-3T3 cells were plated on glass coverslips for 20 h, fixed, and stained with Tks4 antiserum (green) and phalloidin (red). Arrows point to examples of rosettes of podosomes in Src-3T3 cells. Bars,

rected mutagenesis to mutate several candidate tyrosine residues, coexpressed the constructs with Src, immunoprecipitated, and probed for phosphotyrosine. Phosphorylation was reduced when tyrosines 25, 373, and 508 were individually mutated to phenylalanine, and essentially absent when the mutations were combined. Interestingly, tyrosine 25 is in the PX domain and is also described as a phosphorylation site by Phosphosite (www.phosphosite.org). Tyrosine 373 at the amino terminus of the third SH3, and tyrosine 508, in the long linker between the third and fourth SH3 domains, is in a canonical Src SH2 domain binding sequence (YEEI). Despite this, we have been unable to detect an association between Src and Tks4 in cells (unpublished observations). To determine the lipid binding specificity of the Tks4 PX domain, it was fused to GST, expressed in bacteria, purified, and used to probe nitrocellulose filters spotted with phosphatidylinositol lipids (Figure 3). We observed a very similar binding affinity to Tks5, with PI 3-P and PI 3,4P_2 being the preferred lipids, and some association with phosphatidic acid (data not shown).

The Subcellular Localization of Tks4

We used immunofluorescence microscopy to determine the subcellular localization of Tks4 (Figure 4). In 3T3 cells, most cells had a uniform cytoplasmic distribution of Tks4. The occasional cell had more punctate staining. Markers for mitochondria, late endosomes and Golgi failed to fully colocalize with these puncta. Future studies will assess whether the distribution of Tks4 changes with the cell cycle and also further evaluate the nature and significance of this punctate staining. Transformation of 3T3 cells by the activated Src oncogene leads to a dramatic reorganization of the actin cytoskeleton and the formation of rosettes of podosomes. By comparing the localization of F-actin, a known marker for podosomes, and Tks4, we found that the majority of Tks4 was localized to the podosomes of Src-3T3 cells. In this regard then, Tks4 is very similar to Tks5, which is localized to, and required for the formation of, podosome formation and function (Seals *et al*., 2005).

A Role for Tks4 in Podosome Formation and Function

To address the role of Tks4 in podosome formation, we first created Src-3T3 cells stably expressing a shRNA specific for Tks4, and we compared them to cells expressing the empty shRNA vector. We achieved ~90% knockdown of Tks4; this resulted in an equivalent loss of podosome formation (Figure 4). Furthermore, degradation of fluorescent films of gelatin, a hallmark of podosome function, was also inhibited in the knockdown cells. Although these data are strongly supportive of a role for Tks4 in podosome formation and function, we were only able to identify a single shRNA sequence that could effectively reduce Tks4 levels; thus, we could not rule out off target effects. We therefore also took an alternative approach. We isolated primary fibroblasts from mice homozygous for a gene trap in the third intron of Tks4 as well as from wild-type and heterozygous littermates, infected them with a retrovirus encoding activated Src, and tested pools of cells for podosome formation. The Src-expressing wild-type (and heterozygous) MEFs exhibited robust podosome formation (Figure 5). In contrast, the cells homozygous for the gene trap (Tks4$^{-/-}$, which completely lack Tks4 protein expression) had a distinct morphology, and they failed to elaborate podosomes as determined by F-actin staining. However, despite the lack of actin staining, ventral membrane puncta were visualized by staining for the other podosome markers Tks5, cortactin, vinculin, and phosphotyrosine. These data might suggest that, in the absence of Tks4, podosome formation is incomplete. In keeping with this, the Tks4$^{-/-}$ Src-MEFs were unable to degrade fluorescein isothiocyanate (FITC) gelatin, whereas their wild-type counterparts were competent to degrade. To determine whether the changes we saw in podosome formation were due to the acute loss of Tks4, rather than developmental changes in cells derived from Tks4 null mice, we reintroduced Tks4 by infection with a lentivirus encoding

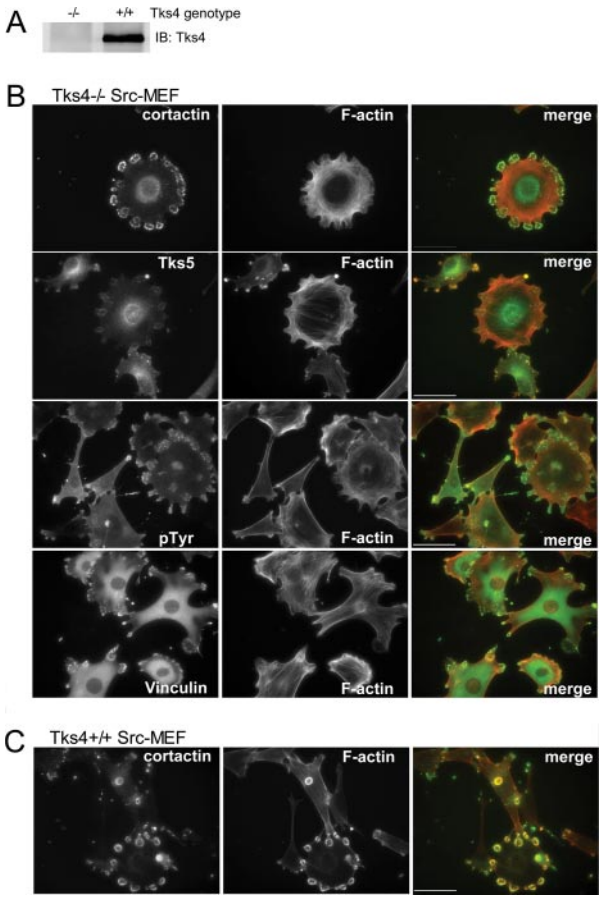

Figure 5. Tks4 null Src-MEFs fail to make functional podosomes. (A) Cell lysates from Src-transformed Tks4$^{-/-}$ and Tks4$^{+/+}$ MEFs were analyzed by SDS-PAGE and immunoblotting with Tks4 antisera. (B) Src-transformed Tks4$^{-/-}$ MEFs were plated on glass coverslips for 20 h, fixed, and stained for the following podosome markers: cortactin, Tks5, phosphotyrosine, vinculin, and F-actin. Bars, 50 μM. (C) Src-transformed Tks4$^{+/+}$ MEFs were plated on glass coverslips for 20 h, fixed, and stained for cortactin and F-actin. Bars, 50 μM.

Figure 4 (cont). 50 μM. (C) Cell lysates from Tks4 shRNA knockdown cells and control shRNA cells were analyzed by SDS-PAGE and immunoblotting with Tks4 antisera. (D) Control and Tks4 knockdown cells were plated on glass coverslips for F-actin (podosome) staining. White arrows point to examples of rosettes of podosomes. One representative image of each cell line is shown. Bars, 50 μM. (E) Quantification of the percentage of cells with rosettes of podosomes from the experiment is shown in D. A minimum of 500 cells were counted from three coverslips. (F) Control and Tks4 knockdown cells were plated on Oregon Green 488 gelatin-coated coverslips for detection of ECM degradation. Bars, 50 μM. (G) Quantification of the degradation of gelatin per cell from the experiment shown in F. Error bars are SEM.

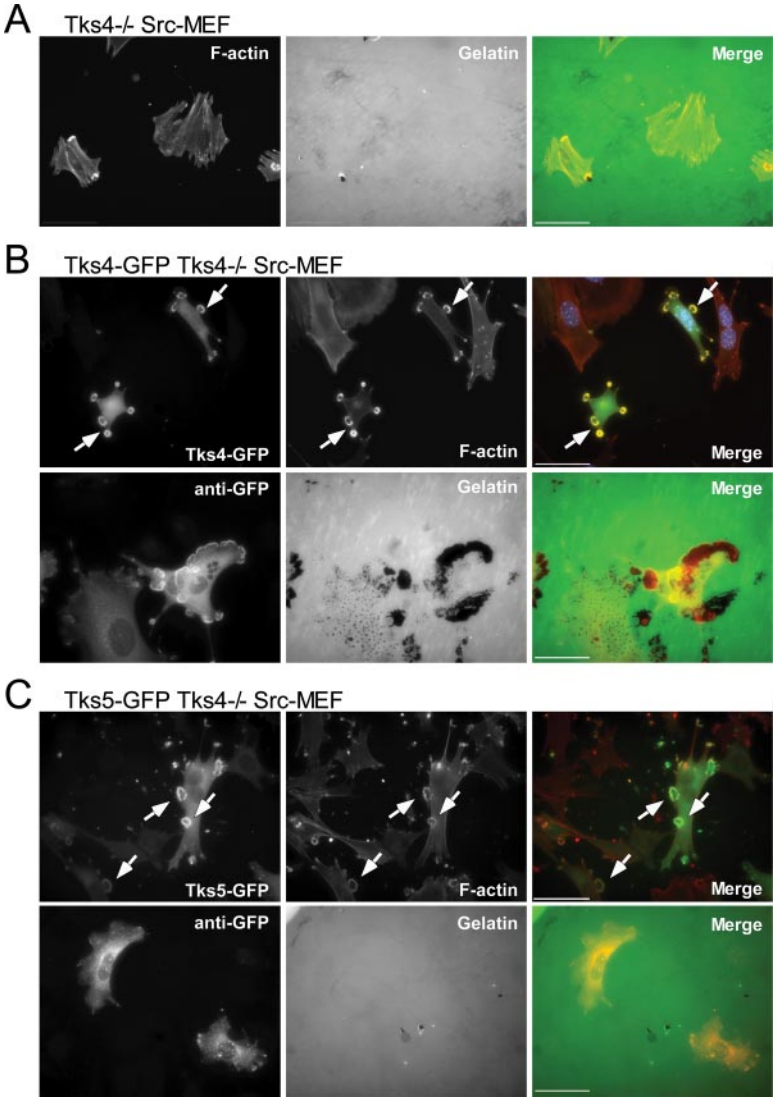

Figure 6. Tks5 expression in Tks4 null Src-MEFs rescues podosome formation, but not function. (A) Src-transformed Tks4$^{-/-}$ MEFs were plated on Oregon Green 488 gelatin-coated coverslips for 4 h and then fixed and F-actin visualized with phalloidin staining. (B) Src-transformed Tks4$^{-/-}$ MEFs were infected with lentivirus encoding Tks4-GFP, plated overnight on glass coverslips, and fixed and stained with phalloidin. White arrows point to examples of rosettes of podosomes. Podosome function (bottom) was investigated by plating cells on Oregon Green 488 gelatin-coated coverslips for 4 h. These cells were fixed in methanol (to denature the GFP and allow visualization of Oregon Green) and stained with anti-GFP antibody to visualize the infected cells. Bars, 50 μM. (C) Src-transformed Tks4$^{-/-}$ MEFs were infected with lentivirus encoding Tks5-GFP and processed as described in B.

Tks4-GFP fusion protein (Figure 6). This treatment restored full podosome formation, as judged by staining for F-actin, as well as FITC-gelatin degradation, in 89% of the infected cells. Together, the results of the shRNA knockdown and the experiments with the Tks4$^{-/-}$ Src-MEFs, strongly suggest that Tks4 is required for functional podosome formation.

Tks4 and Tks5 are very similar adaptor proteins, and both are expressed in Src-3T3 cells and Src-MEFs. We therefore questioned whether they had redundant functions in podosome formation and function. In this scenario, the phenotypes we see in the Tks4 and Tks5 knockdown cells would be due to an overall reduced expression of Tks adaptor proteins. To test this, we increased the expression of Tks5 in the Tks4$^{-/-}$ cells by infecting them with a lentivirus expressing Tks5-GFP (Figure 6). This was sufficient to restore mature podosome formation in these cells, suggesting that these two proteins might indeed have somewhat overlapping functions in recruitment of actin regulators. However, despite the presence of rosettes of podosomes, these cells were not able to degrade FITC-gelatin, unlike the Tks4$^{-/-}$ Src-MEFs rescued with Tks4-GFP. These data are consistent with a unique role for Tks4 in recruiting and/or activating proteases at podosomes. The podosome protein cortactin has recently been implicated in the secretion of matrix metalloproteases. We tested whether Tks4 was also involved in the secretion of the gelatinases MMP2 and MMP9, by using gelatin zymography of conditioned medium, but we could detect no major differences between the Tks4 null cells and those rescued with Tks4 (Figure 7). Another metalloprotease, MT1-MMP, is a key podosome/invadopodia protease that is known to be involved in the control of matrix degradation, perhaps directly or perhaps through activation of MMP2 and MMP9 (Artym *et al*., 2006). In Src-3T3 cells, most MT1-MMP is on intracellular membranes, but using confocal microscopy we could detect that is was also associated with podosome rosettes, as defined by Tks5 staining. However, we could detect no colocalization of Tks5 and MT1-MMP in the Tks4 null cells (Figure 7), suggesting that one role of Tks4 is to recruit MT1-MMP to podosomes.

We identified Tks4 as a Src substrate; therefore, it was of interest to determine whether the tyrosine phosphorylation sites of Tks4 played any role in podosome formation and/or function. Because a lentivirus expressing the triple tyrosine mutant (Y25/373/508F) was not available, we used transfection to introduce either the wild-type or the triple tyrosine mutant into Tks4$^{-/-}$ Src-MEFs. One disadvantage of

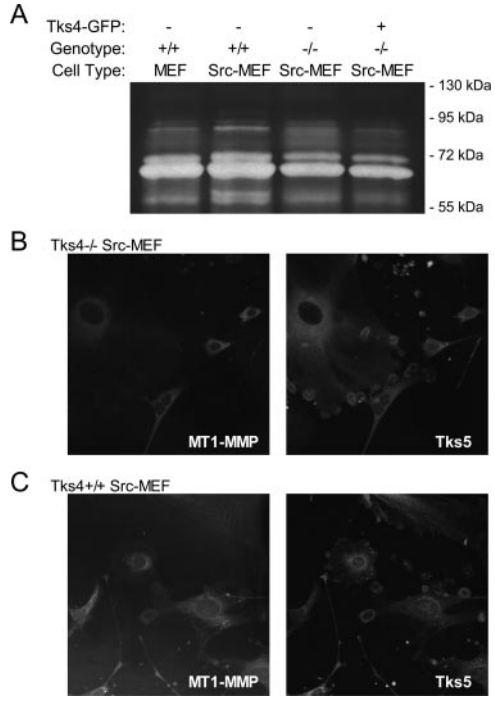

Figure 7. Proteolytic activity of Tks4 null and Tks4 wild-type Src-MEFs. (A) Conditioned media from Src-transformed Tks4$^{-/-}$, Tks4$^{+/+}$, and Tks4-GFP expressing Tks4$^{-/-}$ MEFs were collected and assayed for gelatinase activity. (B) Src-transformed Tks4$^{-/-}$ MEFs were plated on glass coverslips for 20 h, fixed, and stained for MT1-MMP and Tks5, and visualized by confocal microscopy. (C) Src-transformed Tks4$^{+/+}$ MEFs were plated on glass coverslips for 20 h, fixed, and stained for MT1-MMP and Tks5, and visualized by confocal microscopy.

this approach is that only later passage MEFs are able to withstand transfection reagents. And we have found that during continued passage of the null MEFs the level of Tks5 becomes up-regulated and podosomes begin to reform, although importantly matrix degradation is never recovered. We therefore could not quantitate the effect of the triple mutant on podosome formation, although subjectively we did observe increased rosette formation in the transfected cells. We could quantitate matrix degradation ability, however, and we found that although 78% of the cells transfected with wild-type Tks4 degraded matrix, only 29% of the triple mutant-transfected cells were competent for matrix degradation (Figure 8).

DISCUSSION

In this report, we describe the identification and initial characterization of the adaptor protein Tks4, a close relative of the previously described protein Tks5. Like Tks5, Tks4 is broadly expressed, localizes to podosomes of Src-transformed cells, and is required for podosome formation and function. The PX domain of Tks4 has a very similar binding specificity to Tks5 when measured in vitro, and each of the SH3 domains of Tks4 share high sequence identity with four of the SH3 domains of Tks5. The most obvious differences between the two proteins lie in the linker sequences that connect the SH3 domains, and in the Src phosphorylation sites. For Tks4, the linker sequences are highly conserved between mouse and human. However, when this analysis is extended to the zebrafish Tks4 gene, the extent of sequence similarity is much lower. Most of the conserved stretches of sequence in the linkers between the second and third, and third and fourth SH3 domains are proline rich, and they likely represent binding sites for SH3 domain-containing proteins.

We used site-directed mutagenesis of candidate residues to map putative Src phosphorylation sites on human Tks4. One of these sites, Tyr25, which was also detected by Phosphosite, is in the PX domain, and another, Tyr373, is at the beginning of the third SH3 domain. Both of these sites are conserved in *D. rerio*. The third tyrosine phosphorylation site was mapped to Tyr508, in the linker between the third and fourth SH3 domains, and a canonical Src phosphorylation and binding site. Remarkably, this is the only tyrosine residue in any of the linker sequences of Tks4 (in total, >600 amino acids), and it is present in the mouse and human sequences, but not in zebrafish. Our analyses suggest that these tyrosines are required for Tks4 function in podosomes, but it remains to be determined whether it is phosphorylation of these residues which modified function, or whether the amino acid substitution compromised structural integrity. It will also be important to determine whether, and under what conditions, and on which sites, Tks4 is tyrosine phosphorylated in vivo, whether it is a direct substrate of Src, as well as to identify associated proteins.

Like Tks5, we found that the majority of Tks4 had a cytoplasmic distribution in normal fibroblasts. The PX domain of Tks4 is able to bind to PI 3-P, which is found on endosomes (Gillooly *et al*., 2000); yet, only a few cells showed punctate staining that might be consistent with endosomal association. This suggests that the PX domain is not normally available for association with lipids, perhaps because of intramolecular constraints. For example, the PX domain of Tks4 has a proline-rich motif that might cause its association with one of its own SH3 domains. Intramolecular constraints have been shown to occur in the distantly related protein p47^{phox}; in this case, serine phosphorylation of carboxy-terminal sequences renders the amino terminal PX domain competent to bind lipids (Babior, 2002). Because the PX domain of Tks4 can be tyrosine phosphorylated, it will be interesting in the future to determine whether tyrosine phosphorylation plays a role in the lipid binding or subcellular localization of Tks4.

The most intriguing finding that we report here is that in the absence of Tks4, podosome formation is not complete. Thus, we detected several known podosome proteins colocalized in membrane puncta, but these structures were not associated with filamentous actin. A recent study demonstrated that podosome formation in Src-transformed cells starts with the recruitment of a Tks5/Grb2 complex to sites of PI 3,4P_2 accumulation near focal adhesions. This then results in the recruitment of N-WASp to Tks5 and subsequent actin accumulation (Oikawa *et al*., 2008). Our studies show that Tks5 is present in the rudimentary structures present in Tks4$^{-/-}$ cells, yet actin does not accumulate, suggesting that this model is oversimplified. Actin polymerization does occur when Tks5 is overexpressed in Tks4$^{-/-}$ cells, consistent with a hypothesis that under normal circumstances both Tks4 and Tks5 are required for filamentous actin to form, but higher than normal levels of Tks5 can substitute for Tks4. In keeping with this, we have noticed that as the Tks4$^{-/-}$ Src-MEFs are passaged in culture, full podosome formation begins to reappear, coincident with an up-regulation of the level of Tks5 (Buschman and Courtneidge, unpublished observations). We propose that Tks5 can indirectly and directly recruit several proteins, including vinculin and cortactin, which together form a "pre-podosome." The presence of Tks4 is then required to stimulate actin polymerization.

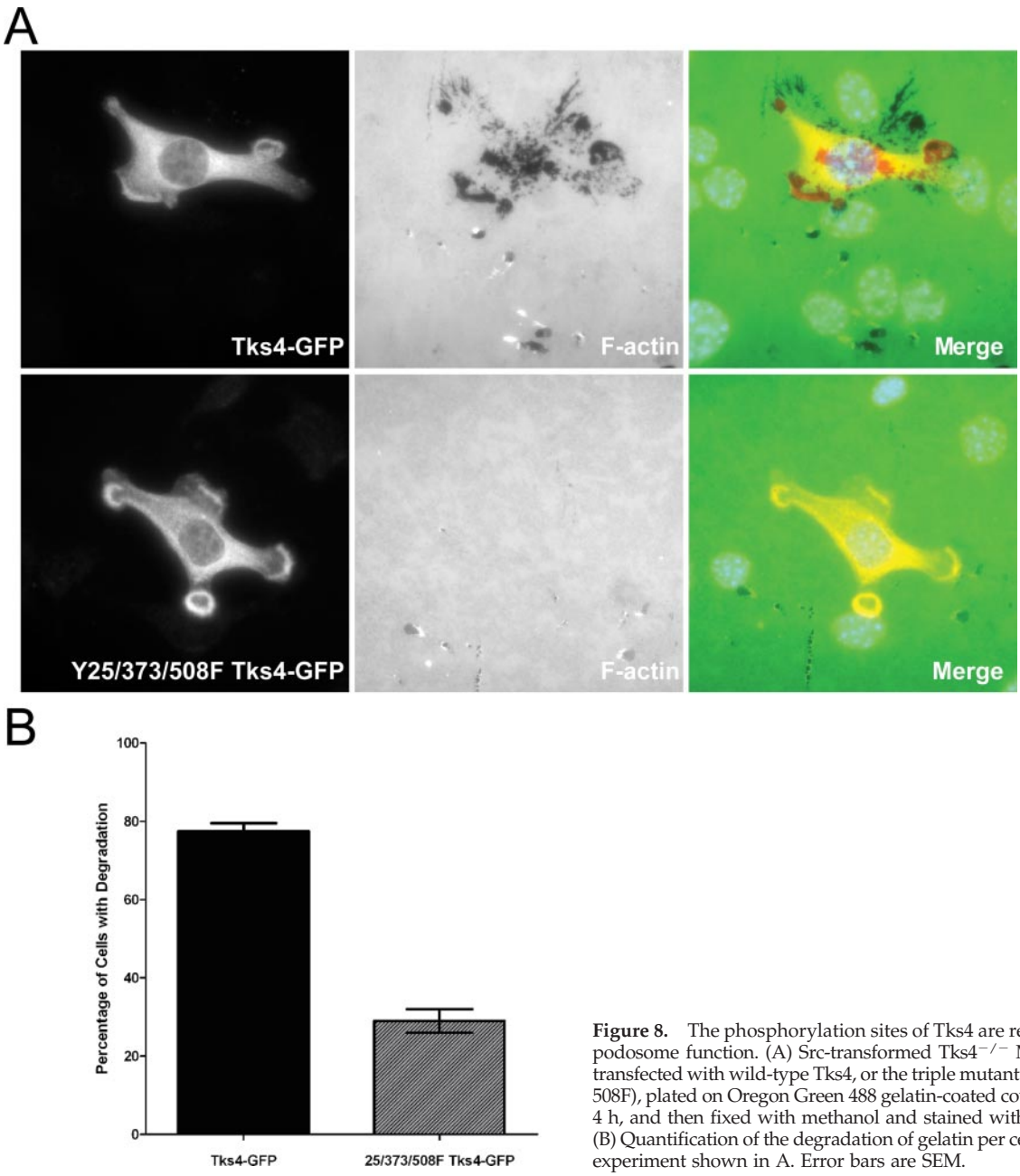

Figure 8. The phosphorylation sites of Tks4 are required for podosome function. (A) Src-transformed Tks4$^{-/-}$ MEFs were transfected with wild-type Tks4, or the triple mutant (Y25/373/508F), plated on Oregon Green 488 gelatin-coated coverslips for 4 h, and then fixed with methanol and stained with anti-GFP. (B) Quantification of the degradation of gelatin per cell from the experiment shown in A. Error bars are SEM.

While continued passage of, or overexpression of Tks5 in, Tks4$^{-/-}$ cells, resulted in the reappearance of podosomes, neither of these conditions were sufficient to restore proteolytic activity. It was recently shown that cortactin is required for protease secretion from invadopodia. In keeping with this, the pre-podosomes in the Tks4$^{-/-}$ Src-MEFs contained cortactin, and secretion of matrix metalloproteases occurred to the same extent as the wild-type cells. Other studies have defined "pre-invadopodia" in human cancer cells, which contain cortactin, low levels of actin, and no MT1-MMP, a transmembrane metalloprotease known to be required for invasive behavior (Artym *et al*., 2006). Pre-podosomes have also been described in vascular smooth muscle cells (Webb *et al*., 2006). In experiments presented here, we show that MT1-MMP is not present in the pre-podosome structures, suggesting that Tks4 is required for its recruitment. In conclusion, the experiments described here reveal a role in podosome formation and function for the new adaptor protein Tks4. Furthermore, the Tks4$^{-/-}$ Src-MEFs should prove a useful tool to study the sequential recruitment of podosome components, and the regulation of proteolytic activity.

ACKNOWLEDGMENTS

We thank Martin Broome for the Src retrovirus vector, Hiroko Kita-Matsuo for Tks4-GFP lentivirus, the Burnham Institute for Medical Research shared resources for lentiviral production, Peter Lock for suggesting the use of B16 cells, and the antibody development scientists at Millipore Bioscience Research Reagents for collaborating with us in the generation of Tks4 antibodies. The Courtneidge laboratory was supported by the National Institutes of Health National Cancer Institute and the Mathers Foundation, and M. B. received support from National Institutes of Health training grant 5T32CA77109-9.

REFERENCES

Abram, C. L., Seals, D. F., Pass, I., Salinsky, D., Maurer, L., Roth, T. M., and Courtneidge, S. A. (2003). The adaptor protein Fish associates with members of the ADAMs family and localizes to podosomes of Src-transformed cells. J. Biol. Chem. *278*, 16844–16851.

Alexander, N. R., Branch, K. M., Parekh, A., Clark, E. S., Iwueke, I. C., Guelcher, S. A., and Weaver, A. M. (2008). Extracellular matrix rigidity promotes invadopodia activity. Curr. Biol. *18*, 1295–1299.

Artym, V. V., Zhang, Y., Seillier-Moiseiwitsch, F., Yamada, K. M., and Mueller, S. C. (2006). Dynamic interactions of cortactin and membrane type 1 matrix metalloproteinase at invadopodia: defining the stages of invadopodia formation and function. Cancer Res. *66*, 3034–3043.

Babior, B. M. (2002). The activity of leukocyte NADPH oxidase: regulation by p47PHOX cysteine and serine residues. Antioxid. Redox. Signal. *4*, 35–38.

Badowski, C., Pawlak, G., Grichine, A., Chabadel, A., Oddou, C., Jurdic, P., Pfaff, M., Albiges-Rizo, C., and Block, M. R. (2008). Paxillin phosphorylation controls invadopodia/podosomes spatiotemporal organization. Mol. Biol. Cell *19*, 633–645.

Baldassarre, M., Pompeo, A., Beznoussenko, G., Castaldi, C., Cortellino, S., McNiven, M. A., Luini, A., and Buccione, R. (2003). Dynamin participates in focal extracellular matrix degradation by invasive cells. Mol. Biol. Cell *14*, 1074–1084.

Bharti, S., Inoue, H., Bharti, K., Hirsch, D. S., Nie, Z., Yoon, H. Y., Artym, V., Yamada, K. M., Mueller, S. C., Barr, V. A., and Randazzo, P. A. (2007). Src-dependent phosphorylation of ASAP1 regulates podosomes. Mol. Cell Biol. *27*, 8271–8283.

Blouw, B., Seals, D. F., Pass, I., Diaz, B., and Courtneidge, S. A. (2008). A role for the podosome/invadopodia scaffold protein Tks5 in tumor growth in vivo. Eur. J. Cell Biol. *87*, 555–567.

Boyce, B. F., Yoneda, T., Lowe, C., Soriano, P., and Mundy, G. R. (1992). Requirement of pp60c-src expression for osteoclasts to form ruffled borders and resorb bone in mice. J. Clin. Invest. *90*, 1622–1627.

Brabek, J., Constancio, S. S., Shin, N. Y., Pozzi, A., Weaver, A. M., and Hanks, S. K. (2004). CAS promotes invasiveness of Src-transformed cells. Oncogene *23*, 7406–7415.

Chen, W. T., Chen, J. M., Parsons, S. J., and Parsons, J. T. (1985). Local degradation of fibronectin at sites of expression of the transforming gene product pp60src. Nature *316*, 156–158.

Chen, W. T., and Wang, J. Y. (1999). Specialized surface protrusions of invasive cells, invadopodia and lamellipodia, have differential MT1-MMP, MMP-2, and TIMP-2 localization. Ann. N Y Acad. Sci. *878*, 361–371.

Clark, E. S., Whigham, A. S., Yarbrough, W. G., and Weaver, A. M. (2007). Cortactin is an essential regulator of matrix metalloproteinase secretion and extracellular matrix degradation in invadopodia. Cancer Res. *67*, 4227–4235.

Cortesio, C. L., Chan, K. T., Perrin, B. J., Burton, N. O., Zhang, S., Zhang, Z. Y., and Huttenlocher, A. (2008). Calpain 2 and PTP1B function in a novel pathway with Src to regulate invadopodia dynamics and breast cancer cell invasion. J. Cell Biol. *180*, 957–971.

Courtneidge, S. A., Azucena, E. F., Pass, I., Seals, D. F., and Tesfay, L. (2005). The SRC substrate Tks5, podosomes (invadopodia), and cancer cell invasion. Cold Spring Harb. Symp. Quant. Biol. *70*, 167–171.

Dowler, S., Currie, R. A., Downes, C. P., and Alessi, D. R. (1999). DAPP *1*, a dual adaptor for phosphotyrosine and 3-phosphoinositides. Biochem. J. *342*, 7–12.

Erpel, T., Superti-Furga, G., and Courtneidge, S. A. (1995). Mutational analysis of the Src SH3 domain: the same residues of the ligand binding surface are important for intra- and intermolecular interactions. EMBO J. *14*, 963–975.

Gatesman, A., Walker, V. G., Baisden, J. M., Weed, S. A., and Flynn, D. C. (2004). Protein kinase Calpha activates c-Src and induces podosome formation via AFAP-110. Mol. Cell. Biol. *24*, 7578–7597.

Gillooly, D. J., Morrow, I. C., Lindsay, M., Gould, R., Bryant, N. J., Gaullier, J. M., Parton, R. G., and Stenmark, H. (2000). Localization of phosphatidylinositol 3-phosphate in yeast and mammalian cells. EMBO J. *19*, 4577–4588.

Gimona, M., Buccione, R., Courtneidge, S. A., and Linder, S. (2008). Assembly and biological role of podosomes and invadopodia. Curr. Opin. Cell Biol. *20*, 235–241.

Linder, S. (2007). The matrix corroded: podosomes and invadopodia in extracellular matrix degradation. Trends Cell Biol. *17*, 107–117.

Linder, S., and Aepfelbacher, M. (2003). Podosomes: adhesion hot-spots of invasive cells. Trends Cell Biol. *13*, 376–385.

Lock, P., Abram, C. L., Gibson, T., and Courtneidge, S. A. (1998). A new method for isolating tyrosine kinase substrates used to identify fish, an SH3 and PX domain-containing protein, and Src substrate. EMBO J. *17*, 4346–4357.

Lowe, C., Yoneda, T., Boyce, B. F., Chen, H., Mundy, G. R., and Soriano, P. (1993). Osteopetrosis in Src-deficient mice is due to an autonomous defect of osteoclasts. Proc. Natl. Acad. Sci. USA *90*, 4485–4489.

Morgenstern, J. P., and Land, H. (1990). Advanced mammalian gene transfer: high titre retroviral vectors with multiple drug selection markers and a complementary helper-free packaging cell line. Nucleic Acids Res. *18*, 3587–3596.

Oikawa, T., Itoh, T., and Takenawa, T. (2008). Sequential signals toward podosome formation in NIH-src cells. J. Cell Biol. *182*, 157–169.

Seals, D. F., Azucena, E. F., Jr., Pass, I., Tesfay, L., Gordon, R., Woodrow, M., Resau, J. H., and Courtneidge, S. A. (2005). The adaptor protein Tks5/Fish is required for podosome formation and function, and for the protease-driven invasion of cancer cells. Cancer Cell *7*, 155–165.

Soriano, P., Montgomery, C., Geske, R., and Bradley, A. (1991). Targeted disruption of the c-src proto-oncogene leads to osteopetrosis in mice. Cell *64*, 693–702.

Tarone, G., Cirillo, D., Giancotti, F. G., Comoglio, P. M., and Marchisio, P. C. (1985). Rous sarcoma virus-transformed fibroblasts adhere primarily at discrete protrusions of the ventral membrane called podosomes. Exp. Cell Res. *159*, 141–157.

Varon, C., Tatin, F., Moreau, V., Van Obberghen-Schilling, E., Fernandez-Sauze, S., Reuzeau, E., Kramer, I., and Genot, E. (2006). Transforming growth factor beta induces rosettes of podosomes in primary aortic endothelial cells. Mol. Cell. Biol. *26*, 3582–3594.

Webb, B. A., Eves, R., and Mak, A. S. (2006). Cortactin regulates podosome formation: roles of the protein interaction domains. Exp. Cell Res. *312*, 760–769.